Effect of Zn and porosity on the biodegradability and Mechanical Properties of Mg-Zn Scaffolds

Zahra-Sadat Seyedraoufi *

[1] *Assistant Professor, Department of Materials Engineering, Karaj Branch, Islamic Azad University, Karaj, Iran*

ARTICLE INFO

Article history:

Received 19 August 2018
Accepted 20 October 2018
Available online 1 December 2018

Keywords:

Porous Scaffold
Mg-Zn
Mechanical Properties
In Vitro biodegradability
Powder Metallurgy

ABSTRACT

In the present research porous Mg-Zn scaffolds with different Zn amount and porosities were synthesized by powder metallurgy process as potential degradable materials for orthopedic applications. The microstructures, composition, mechanical properties and in vitro biodegradability of the scaffolds were investigated. Optic microscopy (OM) images showed that the Mg-Zn scaffolds exhibit homogeneously distributed and interconnected pores with the size of about 150–400 μm. The X-ray diffractometer (XRD) results indicated the formed intermetallics consist of Mg12Zn13 and Mg51Zn20 in the Mg matrix. Compressive tests showed that decrease of porosity and the addition of Zn increases the compressive strength of specimens. Electrochemical tests indicated that with increase of porosity, the corrosion current density of scaffolds increased and Mg-Zn scaffolds synthesized improved the in vitro biodegradability property of the Mg; the best biodegradability property was obtained with 3% Zn and the porosity of about 7% ; further increase of Zn content up 4% deteriorates biodegradability. It is found that the products of immersion in simulated body fluid (SBF) are identified to be HAP, $(Ca,Mg)_3(PO_4)_2$ and $Mg(OH)_2$ and MG63 cells adhere and proliferate on the surface of the scaffolds, making them a promising choice for orthopedic application.

1-Introduction

Significant amount of research efforts have been dedicated to the development of scaffolds for tissue engineering [1]. An ideal bone tissue engineering scaffold must be biocompatible, osteoconductive, and biodegradable, with a high mechanical strength to fulfil the necessary load-bearing functions. Also, it must have interconnected porous networks allowing cell migration, vascularization and nutrient delivery. [1-3]. A bioactive scaffold promotes cell-biomaterial interactions, cell proliferation, adhesion growth, migration, and differentiation. A biodegradable scaffold allows the replacement of biological tissues via physiological extracellular components without leaving toxic degradation products. Its degradation rate should match the rate of new tissue regeneration in order to maintain the structural integrity and to provide a smooth transition of the load transfer from the scaffold to the tissue [3]. The trade-off between the mechanical strength and the porosity is one of the main challenges in designing tissue engineered bone scaffolds. A scaffold must possess sufficient mechanical strength to withstand both the mechanical forces at the scaffold-tissue interface and the implantation

* Corresponding author:
E-mail address: z.seyedraoufi@kiau.ac.ir

procedure [1, 3]. The major challenge is to achieve sufficient initial strength and stiffness and to maintain them during the stage of healing and the scaffold degradation [2-6].

Among the metal implants, Mg and a number of its alloys are effective because of 1) their mechanical properties, which are close to those of human bone, 2) their natural ionic content that has important functional roles in physiological systems, and 3) in vivo biodegradation characteristics in body fluids. Some physical properties of Mg alloys, such as high specific strength and elastic modulus, are closer to those of natural human bone compared to other traditional metal implants; therefore Mg-alloys are potential candidates for biodegradable implants [6-11]. However, their exceedingly high corrosion rates in physiological conditions is the problem with some Mg alloys, which makes their biodegradability to be faster than the time required to heal the bone and the low corrosion resistance in physiological environments can have an adverse effect on the mechanical stability of the implant prior to bone healing [11, 12]. For this reason it is important to decrease the degradation rate of Mg alloys using different techniques such as alloying, purification, surface coating [12- 14].

Elements alloying, as an effective approach to improve the mechanical properties and corrosion resistance, has been studied to develop biodegradable Mg alloys [15]. Zn is selected as the alloying element to achieve the good biocompatibility [15, 16] and Zn is necessary microelement and component of human body. Zn can accelerate the metabolism of cells. The addition of Zn to Mg improves both the corrosion resistance and the mechanical properties of magnesium alloys [15- 17]. The novelty of present study is to produce porous Mg scaffolds containing useful element of Zn without harmful elements such as Ni and Al and the way in which the biodegradability and Mechanical Properties of the Mg scaffolds may be improved. In the present work, porous Mg–Zn scaffolds containing different zinc amounts (1, 2, 3 and 4 wt. %) have been synthesized using a powder metallurgy process and then microstructures, composition, mechanical and in vitro corrosion properties of the scaffolds are investigated.

2- Experimental Procedure

2-1- Synthesis of scaffold

Pure Mg (purity ≥99%, particle size ≤100μm) and pure Zn (particle size ≤45μm, purity ≥99.8%) powders were utilized as starting materials. Urea particles with a purity of 99.9% were used as the space-holder. The particle size of the spacer agent material was in the range of 200-400μm. The mixtures of magnesium and zinc powder were prepared based on 1, 2, 3 and 4 wt. % zinc, while the urea particles were thoroughly added to the above specimens with variable volume contents of 0, 5, 15 and 25%. After weighing magnesium, zinc and urea powders according to the stoichiometric composition, the powders were mixed into glass containers and then mixed with mechanical milling machine for 2 hours. After mixing the starting materials with the space-holder particles, porous Mg-Zn_x (x= 1, 2, 3 and 4 wt. %) samples were prepared via a powder metallurgy method. Details of the fabricated samples are listed in Table 1.

Table 1. Details of the fabricated samples

Sample	)wt.%(Zn	)vol.%(Urea
A_1	1	**0**
A_2	1	**5**
A_3	1	**15**
A_4	1	**25**
B_1	2	**0**
B_2	2	**5**
B_3	2	**15**
B_4	2	**25**
C_1	3	**0**
C_2	3	**5**
C_3	3	**15**
C_4	3	**25**
D_1	4	**0**
D_2	4	**5**
D_3	4	**15**
D_4	4	**25**

The mixed powder was uniaxially pressed at a pressure of 200MPa into green compacts 10 mm in diameter and 10 mm in length. The green compacts were then heat treated to burn out the spacer particles, and to sinter into the porous Mg Scaffolds in a tube furnace under an argon atmosphere. The heat-treatment process consists of two steps, i.e. at 250°C for 4h and 550°C for 2h.

2-2- Characterization

Chemical composition of the specimens was performed by XRD (Philips 1800PW, Netherland) with Cu Kα radiation. Morphology and element composition of the samples were identified by scanning electron microscopy (SEM: Tscan–Vega, China) equipped with energy dispersion spectroscopy facility.

The compressive strength of the composite scaffolds was measured using compression testing of samples with dimensions of d10 mm × 15 mm. The tests were performed with a SANTAM (STM-20, Iran) testing machine at room temperature and a rate of 0.3mm/s. Each result was taken as the mean value of testing on five samples. Pore sizes and morphologies of the porous magnesium specimens were observed using OM. Total porosity (Π) of the porous specimens was measured using gravimetry according to the following equation [18]:

$$\Pi=(1-\rho/\rho_s)\times100\% \quad (1)$$

where ρ_s is the density of the magnesium-zinc specimen evaluated via the immersion method and ρ is the apparent density of the porous magnesium-zinc specimen, which can be measured by the weight-to-volume ratio of the porous specimen.

2-3- Electrochemical measurement

The potentiodynamic polarization curves were obtained using a potentiostat (Autolab/PGSTAT302N) at a constant voltage scan rate of $5mv.s^{-1}$. Experiments were carried out in SBF at 37°C. A three-electrode cell with the samples as the working electrodes was used for the electrochemical measurements. The reference electrode was an Ag–AgCl electrode and the counter electrode was made of platinum. The area of the working electrode exposed to the solution was $0.85cm^2$. The composition and preparation procedure of SBF were as reported in Ref. [19]. The solution was buffered at pH of 7.4 using tris-hydroxymethyl aminomethane ($(HOCH_2)_3CNH_2$) and HCl at 37°C. Each result was taken as the mean value of testing on five samples. The corrosion rate (Pi) of samples obtained from the corrosion current density (i_{corr}) was measured according to the following equation:

$$Pi=22.85i_{corr} \quad (2)$$

2-4- Immersion testing

The immersion testing was carried out in the SBF solution. The pH value of SBF was adjusted to 7.4 with HCl and $(HOCH_2)_3CNH_2$ solutions, and the temperature was kept at 37 °C using water bath. After different immersion periods, the specimens were removed from SBF, rinsed gently with distilled water and dried at 60 °C by drying apparatus. The composition change of the scaffolds after immersion tests was characterized by XRD. An average of three measurements was used for evaluating the pH value of solutions.

2-5- Direct cell adhesion experiment

200 μL cell suspension was seeded onto the as-synthesized, as-deposited and post-treated porous Mg−2Zn scaffolds as well as the control sample at a cell density of 5×104 cell.mL^{-1}. After 8 h culture in a humidified atmosphere with 5% CO^2 at 37 °C in 96-well plates, the parallel samples were fixed in 2.5% glutaraldehyde solution for 2 h at room temperature and rinsed 3 times with phosphate buffer solution (PBS, pH= 7.4), followed by dehydration in a gradient ethanol/ distilled water mixture (50%, 60%, 70%, 80%, 90%, 100%) for 10 min each and dried in hexamethyldisilazane (HMDS) solution. The surface of cell adhered experimental samples was observed by SEM.

3- Results and Discussion

Density and total porosity (Π) of the porous specimens measured using Eq. (1) are listed in Table 2. It is observed that with increasing porosity, the density of samples is reduced. Figure 1 shows the optical micrographs of the B_1, B_2, B_3 and B_4 sintered specimens. It is clear that the pore sizes of the B_1, B_2, B_3 and B_4 specimens are smaller than 100 μm, smaller than 200 μm, 100-300 μm and 200-400 μm, respectively.

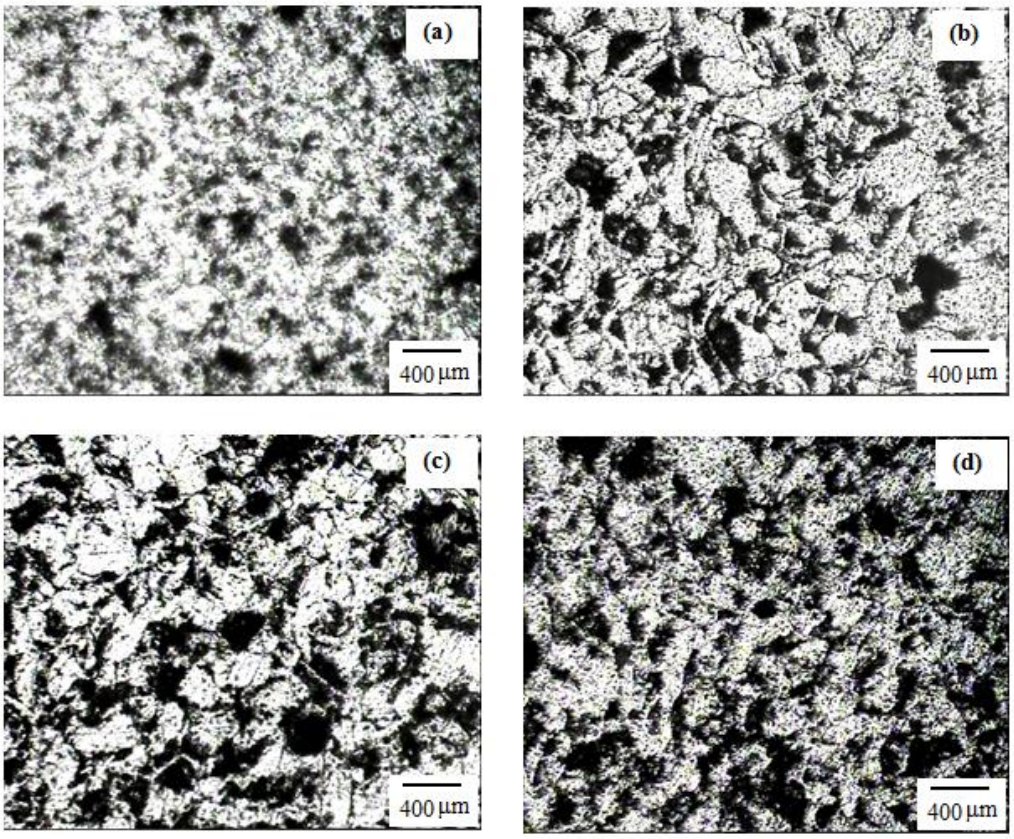

Fig. 1. Optical micrographs of the (a) B_1, (b) B_2, (c) B_3 and (d) B_4 sintered specimens

Table 2. Density, total porosity and compressive strength of the sintered samples

Synthesized scaffold	Density(g/cm^3)	Porosity (%)	The compressive strength (MPa)
A_1	1.62	7	**93**
B_1	1.62	8	**100**
C_1	1.65	7	**108**
D_1	1.64	8	**109**
A_2	1.52	13	**66**
B_2	1.56	12	**64**
C_2	1.59	11	**70**
D_2	1.57	12	**72**
A_3	1.35	23	**26**
B_3	1.36	22	**29**
C_3	1.4	21	**30**
D_3	1.39	22	**32**
A_4	1.17	33	**13**
B_4	1.17	34	**15**
C_4	1.2	32	**18**
D_4	1.21	32	**19**

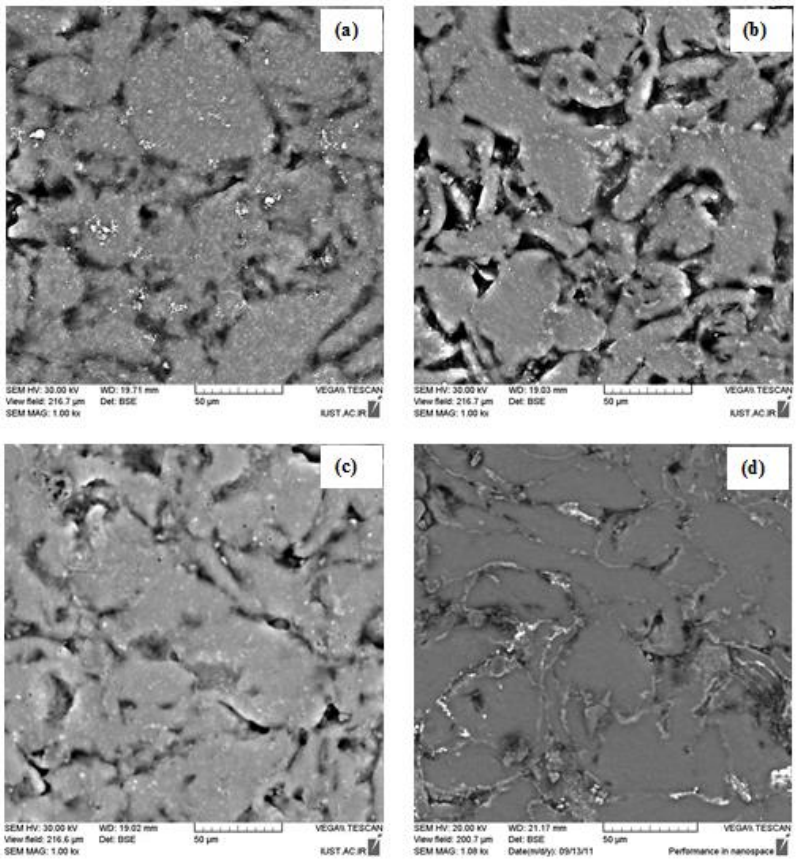

Fig. 2. SEM micrographs of the (a) A_1, (b) B_1, (c) C_1 and (d) D_1 sintered samples.

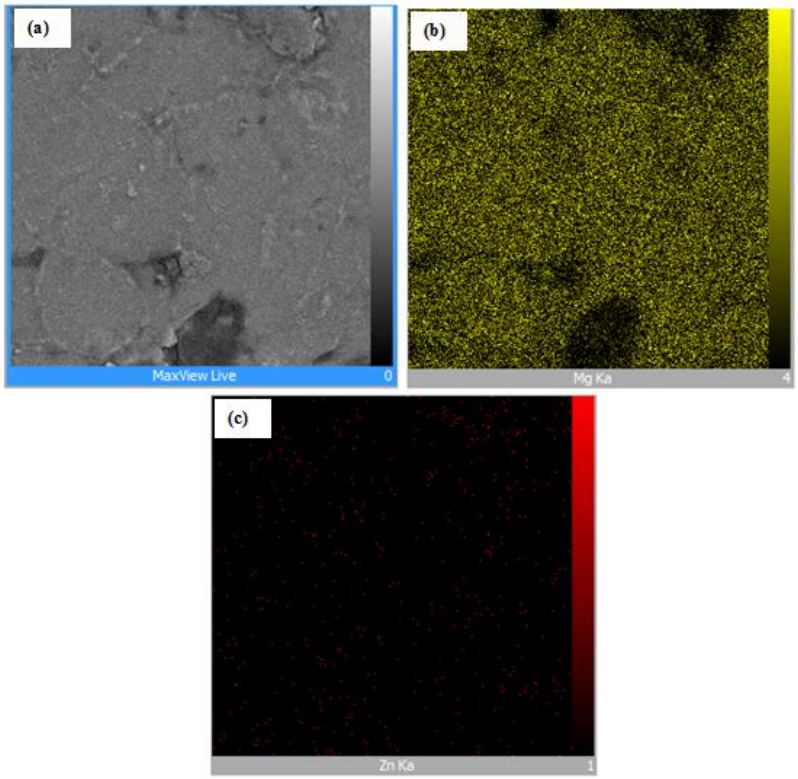

Fig. 3. SEM image (a) and elemental mapping images (b,c) of A_1 sample

It is expected that reaction (3) will occur at about 410 °C. As the sintering temperature increases to about 530 °C, liquid-Zn in the product reacts with Mg to form the molten Mg–Zn alloy [20]. Figure 5 shows the microstructure of the A_2, and D_2 sintered scaffolds. As observed, in the SEM micrograph of D_2 there are three phases. The black, bright and white regions belong to porosity, Mg matrix and Mg-Zn intermetallics. Also, SEM image of A_2 did not show the presence of Mg-Zn intermetallics in the scaffold containing 1 wt. % Zn. Zn element mainly resolves in primary magnesium when Zn content is 1%−2%, which can improve the compressive strength of the scaffold by solid-solution strengthening. When Zn content is 3%, many Mg-Zn intermetallics will precipitate from matrix, which enhances the strength by a dispersion strengthening mechanism [17].

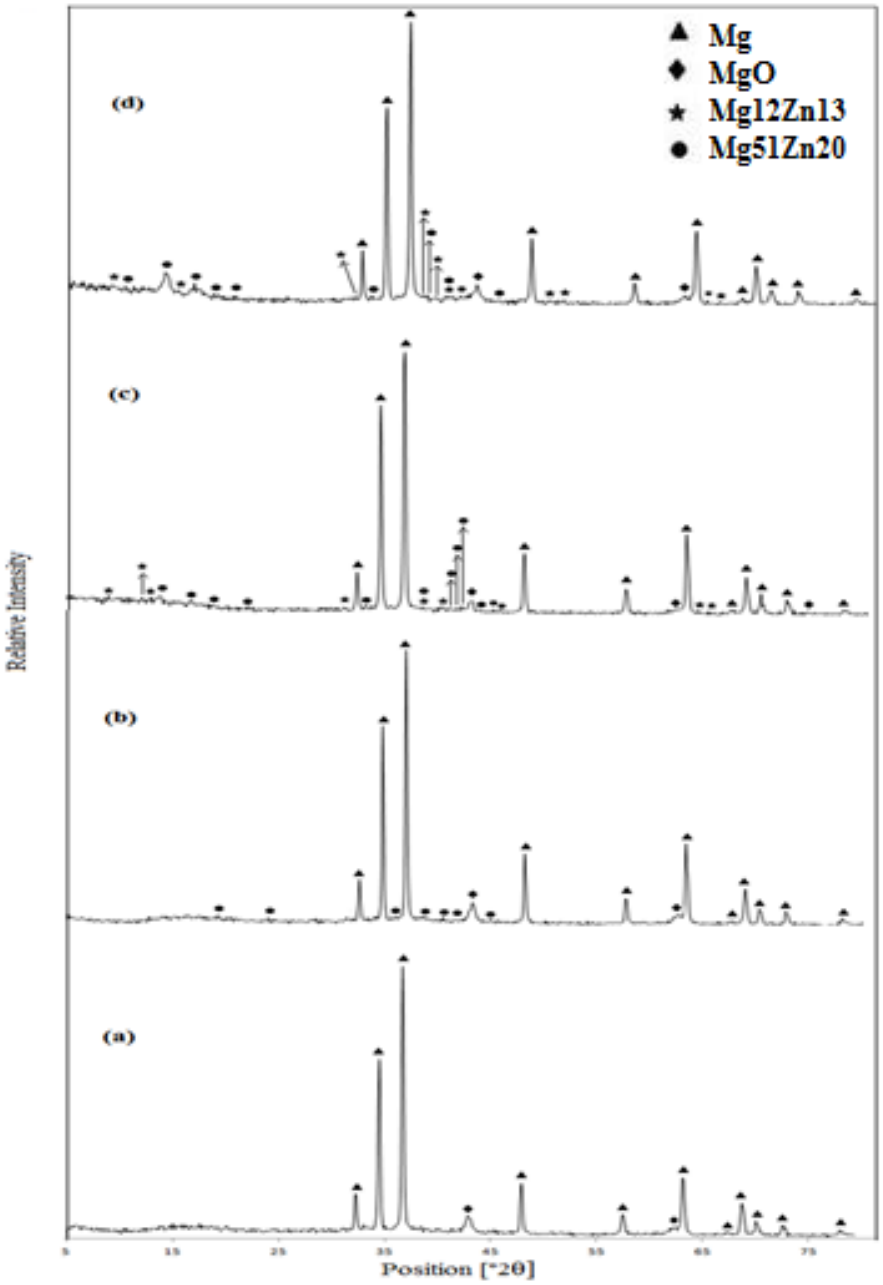

Fig. 4. The XRD patterns of the synthesized scaffolds containing different Zn amounts: (a) A_2, (b) B_2, (c) C_2 and (d) D_2 wt. %

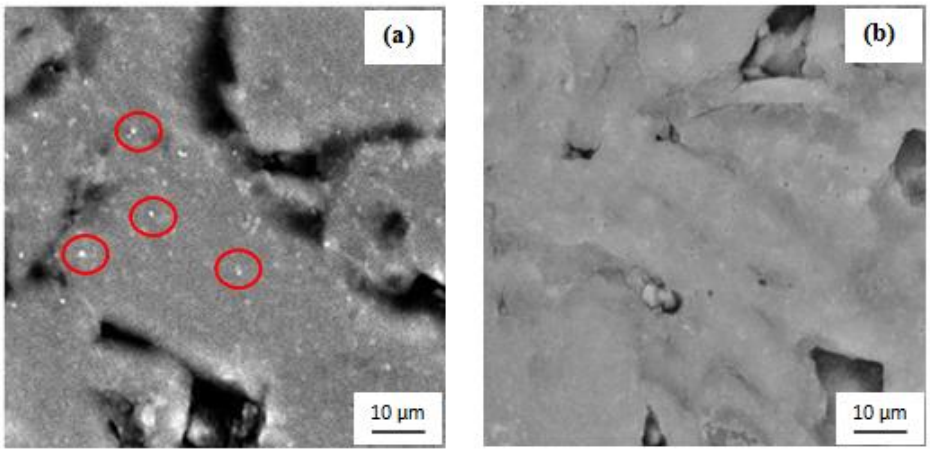

Fig. 5. SEM micrographs of the (a) D_2, and (b) A_2 sintered samples

Figure 6 shows the electrochemical polarization curves of A_1, B_1, C_1 and D_1 sintered scaffolds. Table 3 lists the characteristic parameters obtained from Figure6. The addition of Zn into Mg-Zn scaffolds can obviously move the corrosion potential and the pitting potential to be nobler, indicating that the Zn element can improve the stability of the passivation film and the corrosion resistance. The best corrosion resistance is obtained at 3% Zn. When Zn content exceeds 3% the anti-corrosion property decreases. The change of the pitting potential in Table 4 shows that adding Zn can move the pitting potential to a nobler value to some extent. It was reported that the addition of Zn in magnesium alloy could benefit the formation of a compact passive film [17]. The enrichment of Zn on the surface film can protect the magnesium scaffold from further corrosion. By comparing the Mg-4wt. % Zn scaffold with composite scaffold containing 3 wt. % Zn, the corrosion property is decreased. The probable reason might be that the volume fraction of Mg-Zn phases is higher in Mg-4wt. % Zn scaffold than that in Mg-3wt. % Zn scaffold. When Zn content is up to 3%, many Mg12Zn13 and Mg51Zn20 phases precipitate from matrix, and act as cathode in the corrosion process, which accelerates the corrosion and reduces the anti-corrosion properties of magnesium.

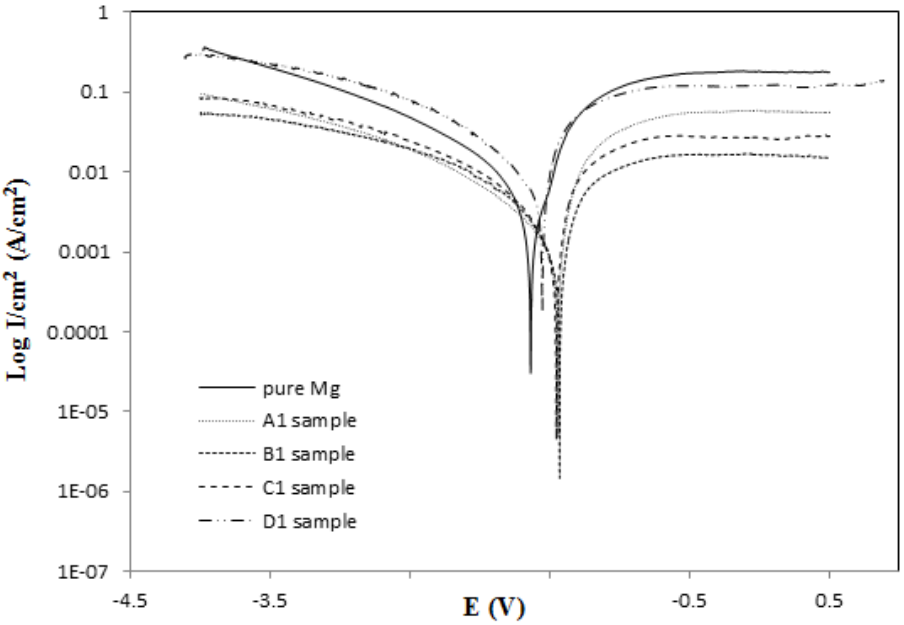

Fig. 6. Electrochemical polarization curves of the Mg-Zn scaffolds containing different Zn amounts

Table 3. Electrochemical parameters of the scaffolds obtained from the polarization curves.

sample	E_{corr} (V)	i_{corr} (A/cm^2)	Pi (A/cm2)
Pure magnesium	-1.64	10.02×10^{-3}	**228.957×10^{-3}**
A_1	-1.44	2.206×10^{-3}	**50.407×10^{-3}**
B_1	-1.429	1.246×10^{-3}	**28.471×10^{-3}**
C_1	-1.453	1.683×10^{-3}	**38.456×10^{-3}**
D_1	-1.554	7.562×10^{-3}	**172.792×10^{-3}**
C_2	-1.464	1.978×10^{-3}	**45.197×10^{-3}**
C_3	-1.475	3.825×10^{-3}	**87.401×10^{-3}**
C_4	-1.501	4.649×10^{-3}	**106.23×10^{-3}**

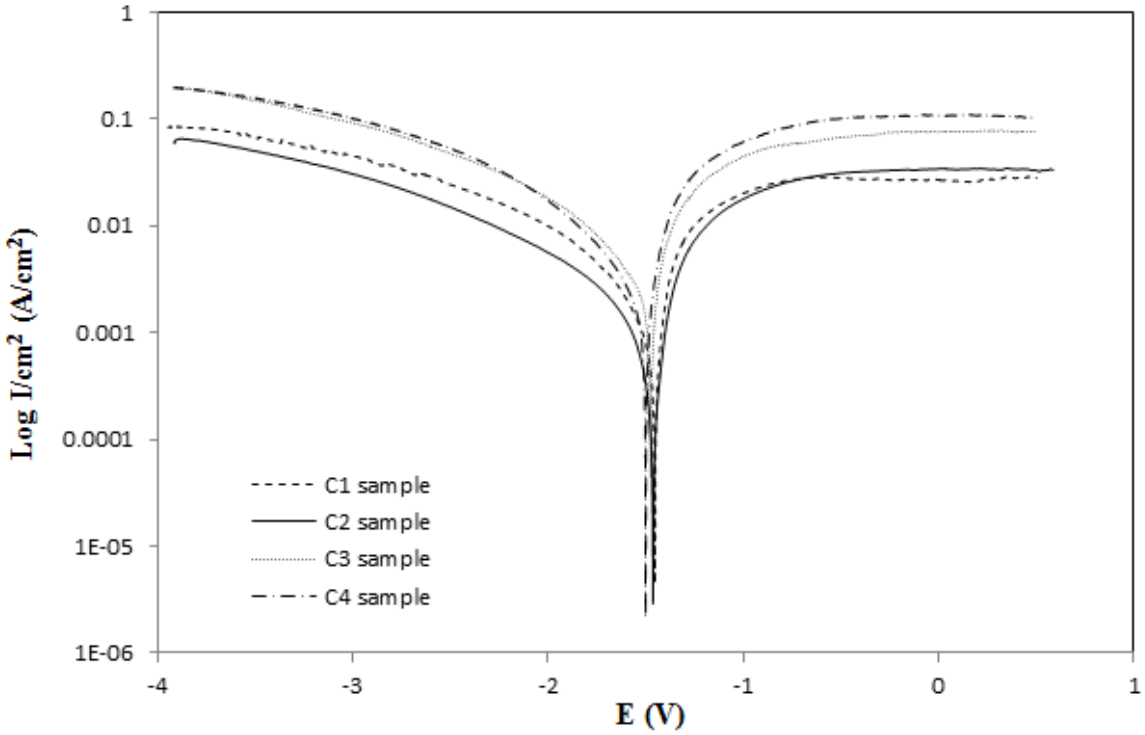

Fig. 7. Electrochemical polarization curves of the Mg-Zn scaffolds containing different porosities.

Figure 7 shows the electrochemical polarization curves of C_1, C_2, C_3 and C_4 sintered scaffolds. It can be seen the scaffolds that have more porosity, are degraded faster. Because the specimens with more porosity have more connecting areas and better condition for transport of the solution, which accelerate the rate of the chemical reactions.

Figure 8 shows the variations of pH value of B_1, B_2, B_3 and B_4 sintered scaffolds in SBF solutions during immersions. It can be seen that the pH values of the solutions immersing all of the porous Mg−Zn specimens tend to increase in the first 9 d, decrease from 9 to 12 d and then keep at a stable pH value of about 9.65. Mg−Zn scaffolds with less porosity exhibit lower change of pH value and degradation rate in body

environment. Mg is converted to Mg^{2+} ions during the degradation process. At the same time, the OH^- ions are released, which causes the pH value of the solutions to increase quickly at early immersion stage. The decrease of pH value from 9 to 12 d should be attributed to formation of the deposited layer containing Ca and P. Actually, the pH value of the solutions will keep at stable level when the balance of the formation and dissolution of the deposit is established after about 12 d.

The formed phases on the surface of C_2 scaffold was characterized after the sample was corroded in SBF for 21 d, as shown in Figure 9. The XRD result confirms that the phases are HAP, $(Ca,Mg)_3(PO_4)_2$ and $Mg(OH)_2$. It can be seen that the formed phase is mainly $Mg(OH)_2$. The $Mg(OH)_2$ peak appears at 2θ of 37.5°, indicating the formation of an alkalized layer. The ions in the SBF solution penetrate the scaffold, leading to further degradation. Ca^{2+} and $(PO_4)^{3-}$ ions near the surface react with OH^- ions caused from Mg corrosion and form HAP.

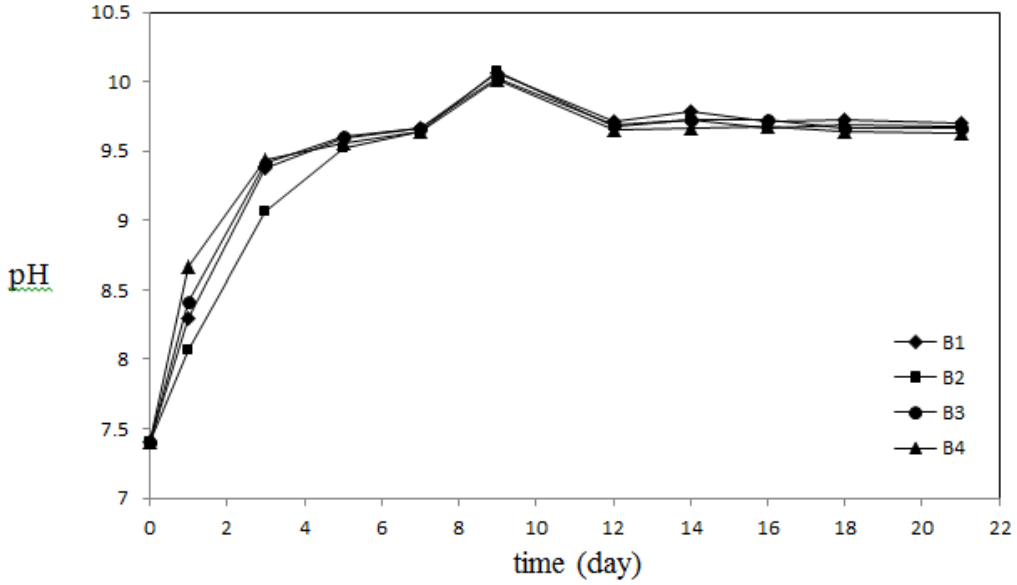

Fig. 8. Change of pH values of SBF solution incubating the Mg-Zn scaffolds containing different porosities during 21 days' immersion.

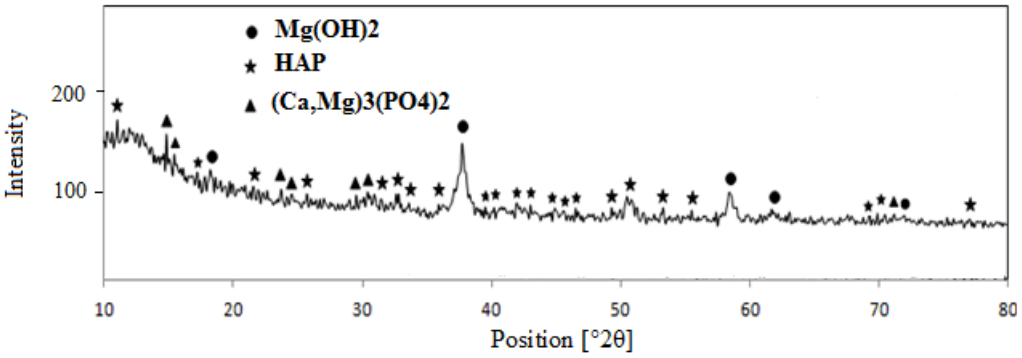

Fig. 9. XRD patterns of the surface of C_2 scaffold after immersion in SBF for 21 d.

A series of studies have demonstrated the interactions between Mg^{2+} and HAP. For instance, there is a critical amount for Mg^{2+}-doped HAP and a higher doping amount will cause the phase transition of HAP [21]. Since Mg^{2+}-incorporated HAP is thermodynamically unstable, the locally accumulated Mg^{2+} may accelerate the decomposition of calcium-deficient hydroxyapatite (Ca-def HAP) by the following reactions: Ca-def

HAP→$(Ca,Mg)_3(PO_4)_2$ or amorphous Ca−P salts (under high Mg^{2+} concentration). It was reported that this calcium magnesium phosphate salt had similar chemical composition to natural bone, which showed good bioactivity and osteoconductivity [22, 23]. MENG et al [22] also reported that osteoconductive minerals containing Ca and P could quickly form on the coatings and remain intact for a period of time which was beneficial to increasing the chances for the formation of an osteointegrated interface after implantation.

Figure 10 shows the morphologies of MG63 cells cultured on the surface of C_2 scaffold for 8 h. Some cells with round shape are observed on the surface after culture for 8 h. Also, it is noted that the microcracks can be seen on surface after culture. In the case of the direct assay, the present study indicates well adhered cells on the surface of scaffold.

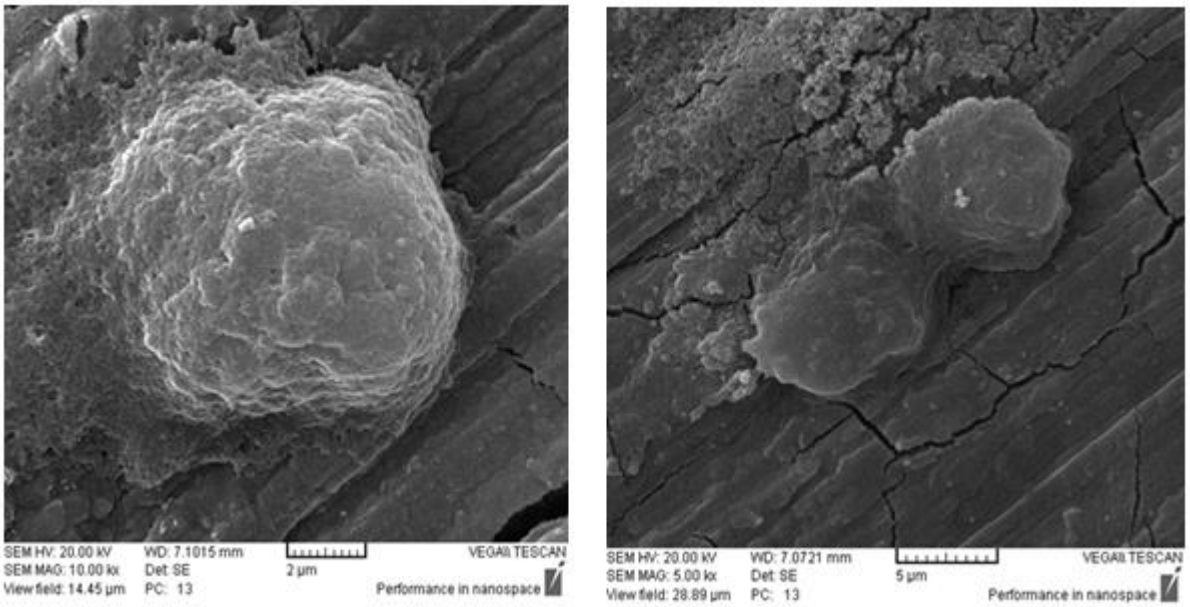

Fig. 10. Morphologies of MG63 cells cultured on the surface of C_2 scaffold for 8 h.

4- Conclusions

Mg-Zn scaffolds with different Zn amount and porosities were successfully fabricated by powder metallurgy process for orthopedic applications. According to results, the Mg-Zn scaffolds exhibit interconnected pores with the approximate size of 150–400 µm. Mechanical properties of porous specimens were investigated by compressive tests focusing on the effects of the Zn and porosity on the strength. The results indicate that the compressive strength of the porous Mg-Zn scaffolds improves with a reduction in volume fraction of porosities and increasing the amount of Zn. Electrochemical tests showed that compared to the pure Mg, Mg-Zn scaffolds synthesized have more appropriate in vitro biodegradability properties; the corrosion current density of scaffolds increased with increase of porosity, and the best biodegradability property was obtained with the porosity of about 7% and 3% Zn. Also, the results showed that the products of immersion in SBF are recognized, to be $Mg(OH)_2$, $(Ca,Mg)_3(PO_4)_2$ and HAP and MG63 cells adhere and proliferate on the surface of the scaffolds, making them a promising selection for orthopedic applications.

References

[1]D. Brahatheeswaran, Y. Yasuhiko, M. Toru, K.D. Sakthi, “Polymeric Scaffolds in Tissue Engineering Application: a Review’, Int. J. Polym. Sci., Vol. 2011, 2011, pp. 1-19.

[2] C.H. Chang, F.H. Lin, T.F. Kuo, H.C. Liu, “Cartilage Tissue Engineering”, Biomed. Eng. Appl. Basis Commun., Vol. 17, 2005, pp. 1–11.

[3] M.V. Risbud, M. Sittinger, “Tissue Engineering: Advances in in Vitro Cartilage Generation”, Trends Biotechnol., Vol. 20, 2002, pp. 351–356.

[4] J. Bonadio, E. Smiley, P. Patil, S. Goldstein, “Localized, Direct Plasmid Gene Delivery in

Vivo: Prolonged Therapy Results in Reproducible Tissue Regeneration", Nat. Med., Vol. 5, 1999, pp. 753–759.
[5] H.Y. Cheung, K.T. Lau, T.P. Lu, D. Hui, "A Critical Review on Polymer-Based Bio-Engineered Materials for Scaffold Development", Compos. Part B, Vol. 38, 2007, pp. 291–300.
[6] A.H. Yusop, A.A. Bakir, N.A. Shaharom, M.R. Abdul Kadir, H. Hermawan, "Porous BiodegradableMetals for Hard Tissue Scaffolds: A Review", Int. J. Biomater., Vol. 2012, 2012, pp. 1-10.
[7] N.E.L. Saris, E. Mervaala, H. Karppanen, J. A. Khawaja, A. Lewenstam, "Magnesium: an Update on Physiological, Clinical and Analytical Aspects", Clin. Chim. Acta, Vol. 294, 2000, pp. 1–26.
[8] J. Vormann, "Magnesium: Nutrition and Metabolism", Mol. Asp. Med., Vol. 24, 2003, pp. 27–37.
[9] T. Okuma, "Magnesium and Bone Strength', Nutr., Vol. 17, 2001, pp. 679–680.
[10] M.P. Staiger, A.M. Pietak, J. Huadmai, G. Dias, "Magnesium and Its Alloys as Orthopedic Biomaterials', Biomater., Vol. 27, 2006, pp. 1728–1734.
[11] F. Witte, V. Kaese, H. Haferkamp, E. Switzer, A. Meyer-Lindenberg, C. Wirth, H. Windhagen, "In Vivo Corrosion of Four Magnesium Alloys and the Associated Bone Response", Biomater., Vol. 26, 2005, pp. 3557–3563.
[12] Z.J. Li, X.N. Gu, S.Q. Lou, Y.F. Zheng, "The Development of Binary Mg–Ca Alloys for Use as Biodegradable Materials within Bone". Biomater., Vol. 29, 2008, pp. 1329–1344.
[13] G.L. Song, "Control of Biodegradation of Biocompatible Magnesium Alloys", Corros. Sci., Vol. 49, 2007, pp. 1696–1701.
[14] S. Gonzáleza, E. Pellicera, J. Fornella, A. Blanquerb, L. Barriosb, E. Ibáñezb, P. Solsonaa, S. Suriñacha, M.D. Baróa, C. Noguésb, J. Sortc, "Improved Mechanical Performance and Delayed Corrosion Phenomena in Biodegradable Mg–Zn–Ca Alloys through Pd-Alloying", Mech. Behav. Biomed. Mater, Vol. 6, 2012, pp. 53–62.
[15] K.U. Kainer, Magnesium Alloys and Their Applications, 1rd ed., Wiley-VCH Verlag GmbH, Frankfurt, 1998, p. 56.
[16] Kh.A. Khalil, "A New-Developed Nanostructured Mg/HAp Nanocomposite by High Frequency Induction Heat Sintering Process", Int. J. Electrochem. Sci., Vol. 7, 2012, pp. 10698 – 10710.
[17] Y. Dong-song, ZH. Erlin, Z. Song-yan, "Effect of Zn on mechanical property and corrosion property of extruded Mg-Zn-Mn alloy", J. Trans. Nonferrous Met. China, Vol.18, 2008, pp. 763-768.
[18] H. Zhuang, Y. Han, A. Feng, "Preparation, mechanical properties and in vitro biodegradation of porous magnesium scaffolds", J. Mater. Sci. Eng. C, Vol. 28, 2008, pp. 1462–1466.
[19] T. Kokubo, H. Takadama, "How useful is SBF in predicting in vivo bone bioactivity", J. Biomater., Vol. 27, 2006, pp. 2907-2915.
[20] C.J. Deng, M.L. Wong, M.W. Ho, P. Yu, H.L. Dickon, "Formation of MgO and Mg–Zn intermetallics in an Mg-based composite by in situ reactions", J. Compos. Part A, Vol. 36, 2005, pp. 551-557.
[21] Y. Song, S.H. Zhang, J. LI, C.H. Zhao, X. Zhang, "Electrodeposition of Ca−P coatings on biodegradable Mg alloy: In vitro biomineralization behavior", J. Acta Biomater. Vol. 6, 2010, pp. 1736−1742.
[22] E.C. Meng, S.K. Guan, H.X. Wang, L.G. Wang, S.J. Zhu, "Effect of electrodeposition modes on surface characteristics and corrosion properties of fluorine-doped hydroxyapatite coatings on Mg−Zn−Ca alloy', J. Appl. Surf. Sci., Vol. 257, 2011, pp. 4811−4816.
[23] M. Yazdimamaghani, M. Razavi, D. Vashaee, K. Moharamzadeh, Aldo R. Boccaccini, L. Tayebi, "Porous magnesium-based scaffolds for tissue engineering", J. Mater. Sci. Eng. C, Vol. 71, 2017, pp. 1253–1266.